Published in final edited form as:
Channels (Austin). 2009 ; 3(1): 32–38.

Synergistic and Antagonistic Interactions between Tetrodotoxin and μ-Conotoxin in Blocking Voltage-gated Sodium Channels

Min-Min Zhang[1], **Jeff R. McArthur**[2], **Layla Azam**[1], **Grzegorz Bulaj**[3], **Baldomero M Olivera**[1], **Robert J French**[2], and **Doju Yoshikami**[1]

[1]Department of Biology, University of Utah, Salt Lake City, Utah, 84112, USA

[2]Department of Physiology & Biophysics, University of Calgary, Calgary, Alberta, Canada T2N 4N1

[3]Department of Medicinal Chemistry, University of Utah, Salt Lake City, Utah, 84108, USA

Abstract

Tetrodotoxin (TTX) is the quintessential ligand of voltage-gated sodium channels (Na_Vs). Like TTX, μ-conotoxin peptides are pore blockers, and both toxins have helped to define the properties of neurotoxin receptor Site 1 of Na_Vs. Here, we report unexpected results showing that the recently discovered μ-conotoxin KIIIA and TTX can simultaneously bind to Site 1 and act in concert. Results with saturating concentrations of peptide applied to voltage-clamped *Xenopus* oocytes expressing brain $Na_V1.2$, and single-channel recordings from brain channels in lipid bilayers, show that KIIIA or its analog, KIIIA[K7A], block partially, with a residual current that can be completely blocked by TTX. In addition, the kinetics of block by TTX and peptide are each affected by the prior presence of the other toxin. For example, bound peptide slows subsequent binding of TTX (an antagonistic interaction) and slows TTX dissociation when both toxins are bound (a synergistic effect on block). The overall functional consequence resulting from the combined action of the toxins depends on the quantitative balance between these opposing actions. The results lead us to postulate that in the bi-liganded Na_V complex, TTX is bound between the peptide and the selectivity filter. These observations refine our view of Site 1 and open new possibilities in Na_V pharmacology.

Keywords

conotoxin; contratoxin; $Na_V1.2$; oocyte; sodium channel; site 1; syntoxin; tetrodotoxin; voltage clamp

Voltage-gated sodium channels (Na_Vs) are responsible for the upstroke of action potentials and play a critical role in electrical signaling in the nervous system. There has been an ongoing interest in ligands to probe the structure and function of these channels. Nine mammalian isoforms of the main pore-forming α-subunit of the channel have been characterized,[1] and ligands that can discriminate among them are useful not only for basic research but also for the development of drugs for diseases such as epilepsy and for pain management.[2, 3] Antagonists of Na_Vs such as tetrodotoxin (TTX) and μ-conotoxins are pore blockers and have been instrumental in the study of these channels.[2, 4] TTX is a small guanidinium alkaloid (Mr = 319), whereas μ-conotoxins are positively-charged peptides of 16 to 25 AA residues sharing a common three disulfide-bridge framework. TTX blocks six of the nine Na_V isoforms with IC_{50}s in the nM range, including $Na_V1.4$ (from skeletal muscle) and $Na_V1.2$ (from brain). In contrast, the best-studied μ-conotoxin, GIIIA, is >100-fold more potent in blocking $Na_V1.4$

Correspondence should be addressed to D.Y. (yoshikami@bioscience.utah.edu).

(IC_{50} = 19 nM in oocyte experiments) than other isoforms, such as $Na_V1.2$ ($IC_{50} \approx 2.7$ μM).[5] Competition-binding studies show that TTX, saxitoxin (STX, another guanidinium alkaloid), and GIIIA all bind to neurotoxin receptor Site 1 of $Na_V1.4$ at the mouth of the permeation pathway for sodium ions.[2, 4, 6, 7]

A residue critical for the functional activity of GIIIA is Arg13.[8] Thus for example, the mutation R13A not only lowers the affinity for $Na_V1.4$ by >80-fold,[9] but also lowers efficacy of block, insofar as the bound mutant peptide incompletely occludes the channel, as manifested by a residual current when single channels are analyzed.[10]

We recently discovered a subset of μ-conotoxins that blocks neuronal Na_Vs as well as, or better than, $Na_V1.4$.[11, 12] The sequence of one of these, KIIIA, is shown below along with that of GIIIA (here, "O" is hydroxyproline, the dashes are spacers to align the Cys's in the two peptides, and * indicates a C-terminal amide).

```
GIIIA  RDCCTOOKKCKDRQCKOQ-RCCA*
KIIIA  --CCN----CSSKWCRDHSRCC*
```

KIIIA had the following intriguing properties that prompted us to examine its interaction with Na_V channels in greater detail. **1**, Single-channel analysis revealed that when KIIIA bound to rat brain sodium channels, most of the unitary current was blocked, but a small residual current remained.[13] The mutant KIIIA[K7A] permits an even larger residual current to flow (JRM & RJF, unpublished; cf. Fig. 5 below). **2**, The homolog of GIIIA's Arg13 in KIIIA is Lys7 (see underlined residues in sequences above). In contrast to GIIIA, single residue replacements of an alanine-walk identified other residues in the C-terminal half of KIIIA that contributed more strongly to high affinity binding than did Lys7.[13] **3**, In contrast to GIIIA, KIIIA showed much stronger binding to $Na_V1.2$ than to $Na_V1.4$.[13] **4**, KIIIA has 6 fewer residues in its N-terminal half than GIIIA, suggesting that it may rely on a different complement of interactions to determine targeting specificity and affinity than does GIIIA.

To further investigate these distinctive features of KIIIA and KIIIA[K7A], we used these peptides together with TTX and examined the dose-dependence and kinetics of the block of sodium current of $Na_V1.2$, expressed in *Xenopus* oocytes, during and after exposure to individual toxins and toxin mixtures. The results indicate that either peptide, KIIIA or KIIIA [K7A], and the alkaloid, TTX, can simultaneously bind to the channel. This conclusion is supported by single-channel recordings of brain Na_V in planar lipid bilayers. Finally, the mutation F385C in $Na_V1.2$, which is near the selectivity filter and renders the channel resistant to TTX, had a small effect on the sensitivity to KIIIA. The overall results are consistent with peptide and TTX being able to form a ternary complex with Site 1 of $Na_V1.2$ and suggest new possibilities in sodium channel pharmacology that could be exploited to substantially expand the repertoire of ligands with which to experimentally probe, or therapeutically target, voltage-gated sodium channels. We introduce the terms "syntoxin" and "contratoxin" that encapsulate two disparate conceptual frameworks engendered by our results.

Results

A residual sodium current persists at saturating concentrations of KIIIA or KIIIA[K7A]

At high peptide concentrations, the dose-response curves of KIIIA and its analog, KIIIA [K7A], were flat, even though 100% block was not achieved (Fig. 1). Experimental determination of the IC_{50}'s of these peptides was problematic because of the slow rates of block by the peptides at concentrations near their expected IC_{50}'s. However, K_d's of the two peptides were calculated from their kinetics (Table 1), and these K_d's were well below the concentrations tested in Figure 1, where the curves were flat. The residual sodium current (rI_{Na}) with KIIIA was 5% of the

control current, and rI_{Na} with KIIIA[K7A] was 23% of control. A similar range of residual, unblocked currents has been observed with conotoxin GIIIA derivatives in both whole-cell14 and single-channel studies.10 The frequency and durations of the partially blocked states are generally consistent with the kinetics of toxin wash in and washout observed in whole-cell recordings. We designate the peptide-bound states of the channel (with residual current) as Na_V•KIIIA or Na_V•KIIIA[K7A], and the TTX-bound state as Na_V•TTX.

TTX blocks the residual current through peptide-bound channels and accelerates peptide dissociation, indicating that bi-liganded complexes can form

The rI_{Na} with either peptide could be completely blocked by TTX (Figs. 2c and 2f). Furthermore, the rate of functional recovery following toxin-washout differed depending on whether the exposure was to TTX alone, peptide alone, or to both peptide and TTX (Fig. 2). The order of ligand-addition (i.e., peptide-first or TTX-first) did not seem to affect the recovery rate (Figs. 2c vs 2d, 2f vs 2g, and Table 1). Thus, these kinetic data, as well as those presented below, argue that bi-liganded complexes can form, which we will refer to as Na_V•TTX•KIIIA and Na_V•TTX•KIIIA[K7A].

TTX blocks rI_{Na} orders of magnitude more slowly than it blocks control I_{Na}

Relatively high [TTX] was used in the experiments illustrated in Figure 2 because the block of rI_{Na} was slow. The rate of block of rI_{Na} was examined over a range [TTX]. The block of rI_{Na} by TTX followed an exponential time course (not illustrated) to yield k_{obs}, and plots of k_{obs} for the block of rI_{Na} as a function of [TTX] are linear (Fig. 3). It is evident from the slopes of the linear regression curves that the apparent k_{on} values for TTX block of Na_V•KIIIA[K7A] and Na_V•KIIIA were reduced relative to the k_{on} for TTX block of Na_V by factors of 10^{-2} and 5×10^{-5}, respectively.

Binding of KIIIA and KIIIA[K7A] to Na_V•TTX appear to occur at rates similar to their binding to unliganded-Na_V

To examine the rate of peptide binding to Na_V already bound with TTX, we exploited the disparity in the rates of recovery from block of Na_V•TTX *vs* Na_V•TTX•peptide; i.e., following toxin-washout, the block produced by either peptide persisted much longer than the block by TTX alone. The time course of recovery during toxin washout following exposure first to a saturating [TTX] (10 μM), then to 10 μM TTX *plus* 1 μM peptide, was well fit by a double exponential (Fig. 4b). The fast component had a rate constant consistent with that of Na_V•TTX and the slow component had a rate constant consistent with that of Na_V•TTX•KIIIA (or Na_VTTX•KIIIA[K7A]). The span of the slower component, when plotted as function of time-of-exposure to peptide, was fit by a single exponential time course (closed circles in Figs. 4c and d) to yield the k_{obs} for the binding of 1 μM peptide to Na_V•TTX. For comparison, also shown is the block of Na_V by 1 μM of each peptide alone (open circles in Figs. 4c and 4d); the presence of TTX reduced the k_{obs} of each peptide by only about 25%.

Single-channel recordings of rat brain Na_V in lipid bilayers show that rI_{Na} with KIIIA[K7A] can be blocked by TTX

In principle, single channel recordings should easily distinguish between conducting states resulting from partial block by a peptide toxin and complete block by TTX, as has been demonstrated for $Na_V1.4$ channels in the simultaneous presence a saxitoxin derivative (dcSTX), and GIIIA[R13Q].[15] For those toxins, blocking events originate only from the unblocked, fully open state, regardless of whether they reflect complete block by dcSTX or partial block by GIIIA[R13Q]. This, along with kinetic analysis, indicated a simple competition between these toxins for the channel vestibule. The macroscopic current analysis of $Na_V1.2$ above suggests a more complex interaction for the smaller KIIIA peptides and TTX, in which

TTX can apparently by-pass the bound peptide, albeit with slow kinetics, and completely block single-channel current. Thus, transitions to a fully blocked state are expected from the peptide-bound, partially blocked state to the non-conducting level. The long bound times of the KIIIA peptides allowed us to observe complete blocking events by adding a high concentration of TTX to the bath, after observing discrete onset of block by the peptide. Such transitions can be recorded from brain Na channels in the presence of KIIIA[K7A] (Fig 5a). Similar events have been recorded from skeletal muscle channels (not illustrated), and these observations offer direct evidence that TTX binds to and blocks the peptide-bound channel.

KIIIA blocks the TTX-resistant mutant $Na_V1.2$[F385C] almost as well as the wild-type channel

The single point mutation of the Phe at position 385 of $Na_V1.2$ to a Cys, resulting in $Na_V1.2$ [F385C], renders the channel insensitive to TTX concentrations up to 10 μM.[16] We constructed the mutant clone and tested TTX concentrations up to 100 μM and found the IC_{50} to be 39 μM (Table 2). Thus, the mutation decreased TTX's affinity 3,000-fold. At these concentrations the rate of block was too fast for our experimental system to determine k_{on}. The k_{off} of TTX for the mutant channel was likewise too fast to be determined. In contrast, the mutation had a much smaller effect on KIIIA's activity: k_{on} was relatively unchanged, and k_{off} was about doubled, resulting in a mere doubling of the K_d (Table 2). Intriguingly, as also indicated in Table 2, the residual current at saturating concentrations of KIIIA was two-fold larger for the mutant channel than for the wild type channel. The weak block of the mutant channel by TTX precluded experiments to see whether TTX blocked the residual current.

Discussion

Formation of the ternary, Na_V•TTX•peptide, complex

Dose-response curves clearly show that an rI_{Na} persists at saturating peptide concentrations (Fig. 1). Residual I_{Na} with the peptides was anticipated from single-channel recordings of rat brain channels incorporated into lipid bilayers, where a small rI_{Na} was observed with the KIIIA-bound channel[13] and an even larger rI_{Na} can be observed with KIIIA[K7A] (Fig. 5a and JRM & RJF, unpublished). However, the observation that TTX can block the (macroscopic) rI_{Na} was not anticipated (Figs. 2c and 2f). The latter observation and the kinetic data reviewed below lead to the conclusion that the two toxins bind to the channels with different affinities and kinetics, and that one molecule of each toxin can bind simultaneously to a single channel to form a bi-liganded complex, Na_V•TTX•peptide (Fig. 5b).

Consistent with this conclusion are observations on single channels incorporated into planar lipid bilayer membranes (Fig 5a). These experiments are challenging, given the intrinsically slow kinetics of the peptide interaction with $rNa_V1.2$[13] and the vast slowing of the TTX interaction when peptide is bound. However, all the conductance states and transitions, which are expected for a scheme in which either or both toxins can bind to the channel were observed: unblocked – state R; KIIIA[K7A]-bound, partially blocked – state A; TTX blocked, non-conducting – state B; and a long duration, non-conducting state entered from state A – the bi-liganded state C.

Implications of the observed off-kinetics

The respective off-rates of KIIIA and KIIIA[K7A] from the mono-liganded Na_V•peptide complex differ from each other by a factor of 10; however, presence of TTX appeared to accelerate the off-rate of KIIIA by about 10-fold but that of KIIIA[K7A] only about 1.7-fold (Table 1). Two factors may contribute to TTX's stronger interactions with KIIIA. First, one would expect an electrostatic repulsion between the positively charged TTX and K7 of KIIIA. Second, even in the absence of TTX, KIIIA[K7A] inherently lacks the normal coupling expected between K7 and negative residues on the channel. When TTX is bound, it would be

expected act as a shield against the native KIIIA toxin's K7-channel interactions, leading to off rates close to those of KIIIA[K7A].

It can be inferred that peptide reduces TTX's off-rate; however, measurements of the off-rates of TTX from Na_V•TTX•peptide in the continuous presence of peptide were not performed, because such experiments require larger quantities of peptide than were available.

The same ternary complex appears to be formed regardless of the order of ligand-addition, insofar as the rate of functional recovery following toxin washout from the ternary complex was essentially the same whether peptide or TTX was added first (Fig. 2 and Table 1).

Implications of the observed on-kinetics

The presence of bound TTX reduced the apparent k_{on} of both peptides modestly and equally (by ~ 25%, Fig. 4) suggesting that TTX does not substantially shield sites on the channel that determine the on-rate of peptide. In stark contrast, the presence of bound peptide drastically reduced the apparent k_{on} of TTX, with KIIIA interfering with TTX binding much more strongly than did KIIIA[K7A] (Fig. 3). In either case however, when TTX does bind, it blocks the rI_{Na} of both Na_V•KIIIA and NaV•KIIIA[K7A] completely, as in the control I_{Na} (Fig. 2). This is consistent with the view that TTX is situated in the same fashion on Na_V in both Na_V•TTX and Na_V•TTX•peptide complexes. These results would be naturally accommodated if the peptide bound to the channel in a manner that still allowed TTX to access its normal binding site, with residue K7 of KIIIA playing an important role in the ease with which TTX can do so.

Implications of interactions between TTX and peptide for biochemical competition-binding studies

As noted above, pre-bound TTX accelerates the off-rate of subsequently-bound peptide, while pre-bound peptide slows the on-rate of subsequently-bound TTX. Thus, in conventional biochemical competition-binding experiments peptide and TTX could appear bind to the channel in a simple competitive fashion unless the experiments were conducted under conditions where 1) binding kinetics were examined over a broad time range, and/or 2) both ligands were labeled, each with a distinctive reporter.

Reaction mechanisms proposed for the formation of the ternary complex

A scheme that takes into account all of our findings is illustrated in a cartoon that also incorporates the possibility that TTX is located between the bound peptide and the channel's narrow selectivity filter, in the ternary complex (Fig 5b). In this scenario, when the peptide is bound first, TTX can “sneak by” and traverse between its non-bound and bound states, but at a considerably slower rate in each direction than it does in the absence of the peptide; thus during toxin-washout, the rate limiting factor for recovery of function of the ternary complex is the rate at which the peptide comes off. The presence of TTX reduces the peptide's affinity, so activity is recovered more rapidly from Na_V•TTX•peptide than from Na_V•peptide. The scheme is also supported by the observation that the F385C mutation of $Na_V1.2$, which drastically reduces affinity for TTX, minimally affected KIIIA's activity. At the same time, the mutation doubled the residual I_{Na} seen at saturating [KIIIA] (Table 2). This behavior with the mutant channel is consistent with KIIIA binding close to the selectivity filter.

Our results support the view that a neurotoxin receptor site may be considered as a macrosite composed of an amalgamation of microsites.[17] In the present case of (macro)Site 1 of $Na_V1.2$, TTX occupies one set of microsites, the peptide another set of microsites, and a third set of microsites might exist that is accessible to both toxins when each binds in the absence of the other. We cannot rule out the possibility that KIIIA is binding at a location distinct from, but

allosterically linked to, the site where TTX binds. However, our working assumption of a single multivalent macrosite seems more parsimonious.

Is our conclusion that Site 1, at least that of $Na_V1.2$, can accommodate both TTX and KIIIA consistent with current structural models of Site 1? Recent experiments with $Na_V1.4$ indicate that TTX binds via a cation-pi interaction, where the cationic guanidinium group of TTX associates with the aromatic ring of the Tyr residue 401 (homologous to Phe 385 of $Na_V1.2$) that is next to Asp of the selectivity filter in domain I of the channel.[18] The sensitivity of $Na_V1.4$ to TTX is drastically decreased by the Y401C mutation (IC_{50} increased 43- to >3125-fold);[19, 20] yet that mutation reduces GIIIA's affinity only 2- to 4-fold.[20, 21] These observations are echoed by our results with KIIIA and $Na_V1.2$[F385C], and together they suggest that, in contrast to TTX, μ-conotoxins generally dock at a more superficial site in the outer vestibule of the channel,[2, 22] raising the possibility that KIIIA might allow TTX, albeit with the observed reduced probability and association rate, to pass by the peptide and bind at or near its normal site deeper in the vestibule. This contrasts with the case of the STX analog, dcSTX, and the bulkier conotoxin derivative, GIIIA(R13Q), for which binding is mutually exclusive on $Na_V1.4$.[15]

TTX and KIIIA act as “syntoxins”

Given that our present data indicate that peptide (KIIIA or KIIIA[K7A]) and TTX can cohabit Site 1, with functional consequences different from those when each toxin acts alone, they might be thought of as “syntoxins”. The expression, syntoxin, encapsulates the notion that two toxins can act in concert. In the case of KIIIA (or KIIIA[K7A]) and TTX, the concerted action has mixed synergistic and antagonistic effects: presence of peptide slows both dissociation and association of TTX (the former action enhances, while the latter diminishes, TTX affinity); reciprocally, the presence of TTX accelerates peptide dissociation.

It will be interesting to further test for syntoxin interactions using different ligands and receptors. Possible ligands include other μ-conotoxins, such as SIIIA, which has 6 more residues than KIIIA;[11] other guanidinium alkaloids, including STX, which has 94% the molecular mass of TTX but with two, instead of only one, guanidinium groups; possible targets, include $Na_V1.4$, whose binding with GIIIA has received extensive scrutiny (see ref. 22 for a recent report). Positive findings in this endeavor would suggest new possibilities in sodium channel pharmacology. A syntoxin pair, in context, may be considered as a self-assembling, two-part toxin, where one member has a motif of a guanidinium alkaloid, and the other member has one of a μ-conopeptide. Pairs of members with each motif could be readily tested, in a mix-and-match fashion, for activity against different Na_V subtypes. Syntoxin pairs, themselves, might be exploited to substantially expand the repertoire of pharmacological actions targeted at specific subtypes of voltage-gated sodium channels. Furthermore, those pairs yielding the highest affinities might be subsequently engineered into covalently linked, bivalent ligands with the expectation that some could achieve even greater affinity than the corresponding non-linked pair (see e.g., ref. 23).

A modified μ-conotoxin with a large residual I_{Na} could serve as a “contratoxin”

Quite apart from the syntoxin properties of KIIIA and KIIIA[K7A], our results show that the peptide's structure can be engineered to attenuate its efficacy; that is, to block a smaller faction of the single-channel current when it binds. Thus, a ligand with high affinity and low (or ideally no) efficacy could be used as a “contratoxin.” For example, in the case of sodium channels, a ligand with high affinity for Site 1 but minimal ability to block the pore, could act as a contratoxin against other toxins that target Site 1, such as TTX and functionally active μ-conotoxins. Note that the action of a contratoxin is distinct from that of an antitoxin, which is an antibody that neutralizes a toxin by binding to the toxin; in contrast, a contratoxin prevents

a toxin's action by binding to the toxin's receptor. A contratoxin could not only serve as an antidote to TTX, but (depending on its specificity for different Na_Vs) could also be used in conjunction with TTX to sharpen the latter's specificity.

Methods

Wild type and mutant $Na_V1.2$ clones

The cDNA for rat $Na_V1.2$ was kindly provided by Alan Goldin. The point mutant, $Na_V1.2$ [F385C], where Phe 385 is mutated to Cys, was prepared from the wild type clone as follows. Forward and reverse primers containing the mutation were designed with the following sequences: forward, 5′ctcatgactcaagactgttgggaaaacctttatc3′; reverse, 5′ gataaaggttttcccaacagtcttgagtcatgag3′. The mutagenic primers were extended and incorporated by PCR using Finnzyme Phusion™ High-Fidelity DNA polymerase (New England Biolabs, Ipswich, MA). The methylated, non-mutated parental cDNA was digested with *Dpn I*. The mutated DNA was transformed into DH5α competent cells, and positive colonies were selected based on tetracycline-resistance. Plasmid was isolated using the Qiaprep Spin Miniprep kit (Qiagen, Valencia, CA) and sequenced to ascertain the incorporation of the desired mutation. Capped cRNA for $Na_V1.2$[F385C] was made using the mMessage mMachine *in vitro* transcription kit (Ambion, Austin, TX), following linearization of the plasmid and subsequent transcription with T7 RNA polymerase. The final product was purified using the Qiagen RNeasy kit.

Oocyte Electrophysiology

Oocytes expressing mutant and wild type $Na_V1.2$ were prepared and two-electrode voltage clamped essentially as previously described.[13] Briefly, oocytes were placed in a 30 μL chamber containing ND96 and two electrode voltage clamped with a holding potential of −80 mV. To activate Na channels, the membrane potential was stepped to −10 mV for 50 ms every 20 sec. The oocytes were exposed to toxin in static baths to conserve material. During toxin-washout, the oocyte chamber was perfused at 1.5 ml/min for 20 sec, then at 0.5 ml/min thereafter. Recordings were done at room temperature (~21 °C).

Single-channel Recordings

Membrane vesicles were isolated from adult rat fore-brains as described previously.[24] Membrane vesicles were incubated with batrachotoxin (1 μM in ethanol) then pipetted directly over a horizontal bilayer (4PE:1PC) in symmetric solutions (200mM NaCl, 10mM MOPS, 0.1mM EDTA, pH 7.0) and incorporation was detected as a step increase in current (~1 pA) at 60 mV. Orientation of the channel was deduced as an increase in closure frequency at −70 mV and 2 μM KIIIA[K7A] toxin with 50 nM TTX was then perfused into the “extracellular” chamber (2 × 400 μL). Steady-state recordings at +40 mV were collected; upon block by the peptide, TTX (10 μM) was added.

Toxins

μ-Conopeptides were synthesized as previously described[13]. TTX was obtained from Alomone Labs.

Data Analysis

Off-rate constants (k_{off}'s) were determined from single-exponential fits of peak sodium current following toxin washout, unless otherwise indicated. Observed rate constants (k_{obs}'s) were obtained by single exponential fits of peak sodium current following toxin addition, and on-rate constants (k_{on}) were obtained from slopes of k_{obs} *versus* [toxin].[25]

Acknowledgments

We thank Alan Goldin, UCLA, for providing the Nav1.2 clone and Aleksandra Walewska for synthesizing conotoxins. This work was supported by National Institutes of Health grants GM 48677 and NS055845. Work in the French laboratory was supported by the Heart & Stroke Foundation of Alberta, NWT & Nunavut.

References

1. Catterall WA, Goldin AL, Waxman SG. International Union of Pharmacology. XLVII. Nomenclature and structure-function relationships of voltage-gated sodium channels. Pharmacological reviews 2005;57:397–409. [PubMed: 16382098]
2. French RJ, Terlau H. Sodium channel toxins--receptor targeting and therapeutic potential. Curr Med Chem 2004;11:3053–64. [PubMed: 15578999]
3. Wood JN, Boorman JP, Okuse K, Baker MD. Voltage-gated sodium channels and pain pathways. Journal of neurobiology 2004;61:55–71. [PubMed: 15362153]
4. Cestele S, Catterall WA. Molecular mechanisms of neurotoxin action on voltage-gated sodium channels. Biochimie 2000;82:883–92. [PubMed: 11086218]
5. Safo P, Rosenbaum T, Shcherbatko A, Choi DY, Han E, Toledo-Aral JJ, Olivera BM, Brehm P, Mandel G. Distinction among neuronal subtypes of voltage-activated sodium channels by mu-conotoxin PIIIA. J Neurosci 2000;20:76–80. [PubMed: 10627583]
6. Al-Sabi A, McArthur J, Ostroumov V, French RJ. Marine toxins that target voltage-gated sodium channels. Mar Drugs 2006;4:157–92.
7. Catterall WA. Neurotoxins that act on voltage-sensitive sodium channels in excitable membranes. Annu Rev Pharmacol Toxicol 1980;20:15–43. [PubMed: 6247957]
8. Sato K, Ishida Y, Wakamatsu K, Kato R, Honda H, Ohizumi Y, Nakamura H, Ohya M, Lancelin JM, Kohda D, et al. Active site of mu-conotoxin GIIIA, a peptide blocker of muscle sodium channels. The Journal of biological chemistry 1991;266:16989–91. [PubMed: 1654319]
9. Becker S, Prusak-Sochaczewski E, Zamponi G, Beck-Sickinger AG, Gordon RD, French RJ. Action of derivatives of mu-conotoxin GIIIA on sodium channels. Single amino acid substitutions in the toxin separately affect association and dissociation rates. Biochemistry 1992;31:8229–38. [PubMed: 1326324]
10. Hui K, Lipkind G, Fozzard HA, French RJ. Electrostatic and steric contributions to block of the skeletal muscle sodium channel by mu-conotoxin. The Journal of general physiology 2002;119:45–54. [PubMed: 11773237]
11. Bulaj G, West PJ, Garrett JE, Watkins M, Zhang MM, Norton RS, Smith BJ, Yoshikami D, Olivera BM. Novel conotoxins from Conus striatus and Conus kinoshitai selectively block TTX-resistant sodium channels. Biochemistry 2005;44:7259–65. [PubMed: 15882064]
12. Zhang MM, Fiedler B, Green BR, Catlin P, Watkins M, Garrett JE, Smith BJ, Yoshikami D, Olivera BM, Bulaj G. Structural and functional diversities among mu-conotoxins targeting TTX-resistant sodium channels. Biochemistry 2006;45:3723–32. [PubMed: 16533055]
13. Zhang MM, Green BR, Catlin P, Fiedler B, Azam L, Chadwick A, Terlau H, McArthur JR, French RJ, Gulyas J, Rivier JE, Smith BJ, Norton RS, Olivera BM, Yoshikami D, Bulaj G. Structure/function characterization of micro-conotoxin KIIIA, an analgesic, nearly irreversible blocker of mammalian neuronal sodium channels. The Journal of biological chemistry 2007;282:30699–706. [PubMed: 17724025]
14. French, RJ.; Horn, R. Shifts of macroscopic current activation in partially blocked sodium channels Interaction between the voltage sensor and a mu-conotoxin. In: Latorre, R.; Saez, JC., editors. From Ion Channels to Cell-to-Cell Conversations. New York: Plenum Press; 1997. p. 67-89.
15. French RJ, Prusak-Sochaczewski E, Zamponi GW, Becker S, Kularatna AS, Horn R. Interactions between a pore-blocking peptide and the voltage sensor of the sodium channel: an electrostatic approach to channel geometry. Neuron 1996;16:407–13. [PubMed: 8789955]
16. Heinemann SH, Terlau H, Imoto K. Molecular basis for pharmacological differences between brain and cardiac sodium channels. Pflugers Arch 1992;422:90–2. [PubMed: 1331981]
17. Olivera BM, Rivier J, Scott JK, Hillyard DR, Cruz LJ. Conotoxins. The Journal of biological chemistry 1991;266:22067–70. [PubMed: 1939227]

18. Santarelli VP, Eastwood AL, Dougherty DA, Horn R, Ahern CA. A cation-pi interaction discriminates among sodium channels that are either sensitive or resistant to tetrodotoxin block. The Journal of biological chemistry 2007;282:8044–51. [PubMed: 17237232]

19. Backx, PH.; Yue, DT.; Lawrence, JH.; Marban, E.; Tomaselli, GF. Science. Vol. 257. New York, NY: 1992. Molecular localization of an ion-binding site within the pore of mammalian sodium channels; p. 248-51.

20. Chen LQ, Chahine M, Kallen RG, Barchi RL, Horn R. Chimeric study of sodium channels from rat skeletal and cardiac muscle. FEBS letters 1992;309:253–7. [PubMed: 1325372]

21. Li RA, Tsushima RG, Kallen RG, Backx PH. Pore residues critical for mu-CTX binding to rat skeletal muscle Na+ channels revealed by cysteine mutagenesis. Biophysical journal 1997;73:1874–84. [PubMed: 9336183]

22. Choudhary G, Aliste MP, Tieleman DP, French RJ, Dudley SC Jr. Docking of mu-conotoxin GIIIA in the sodium channel outer vestibule. Channels 2007;1:344–52. [PubMed: 18690041]

23. Rao, J.; Lahiri, J.; Isaacs, L.; Weis, RM.; Whitesides, GM. Science. Vol. 280. New York, NY: 1998. A trivalent system from vancomycin.D-ala-D-Ala with higher affinity than avidin.biotin; p. 708-11.

24. Krueger BK, Worley JF 3rd, French RJ. Block of sodium channels in planar lipid bilayers by guanidium toxins and calcium. Are the mechanisms of voltage dependence the same? Annals of the New York Academy of Sciences 1986;479:257–68. [PubMed: 2433995]

25. West PJ, Bulaj G, Garrett JE, Olivera BM, Yoshikami D. Mu-conotoxin SmIIIA, a potent inhibitor of tetrodotoxin-resistant sodium channels in amphibian sympathetic and sensory neurons. Biochemistry 2002;41:15388–93. [PubMed: 12484778]

Abbreviations

GIIIA	μ-conotoxin GIIIA
I_{Na}	sodium current
KIIIA	μ-conotoxin KIIIA
KIIIA[K7A]	μ-conotoxin KIIIA[K7A]
Na_V	voltage-gated sodium channel
Na_V•KIIIA	the binary complex of Na_V with bound KIIIA
Na_V•KIIIA[K7A]	the binary complex of Na_V with bound KIIIA[K7A]
Na_V•TTX	the binary complex of Na_V with bound TTX
Na_V•TTX•KIIIA	the ternary complex of Na_V with bound TTX and KIIIA
Na_V•TTX•KIIIA[K7A]	the ternary complex of Na_V with bound TTX and KIIIA[K7A]
rI_{Na}	residual sodium current

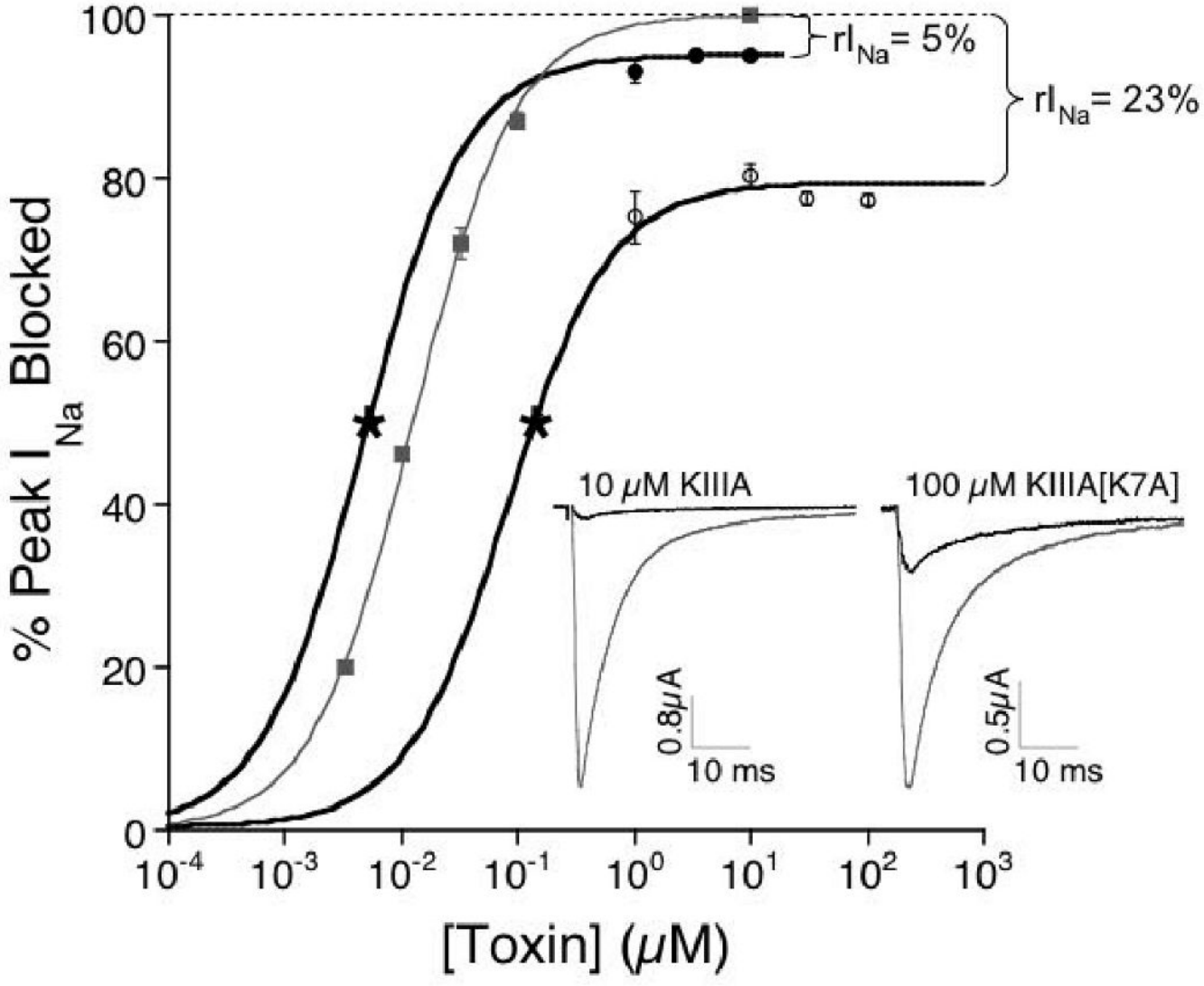

Figure 1.

Steady state dose-response curves reveal a residual Na current (rI_{Na}) at saturating peptide concentrations. Data (KIIIA, closed circles; KIIIA[K7A], open circles; TTX, closed squares) were obtained with oocytes expressing $Na_V1.2$ as described in Methods. Small k_{on} prevented acquisition of steady-state data at [peptide] in the vicinity of K_d, represented by asterisk, obtained from k_{off}/k_{on} (Table 1). Solid lines represent fit of data, including asterisks, to the Langmuir isotherm, $Y = 100 \bullet \text{plateau}/[1 + (IC_{50}/[\text{toxin}])]$. Plateau (i.e., Y-axis value at saturating [toxin]) was 95 ± 3% for KIIIA and 77 ± 1% for KIIIA[K7A] and 100% for TTX. Insets, representative current recordings in the absence (control, gray traces) and presence (black traces) of saturating concentrations of KIIIA (10 μM, left) and KIIIA[K7A] (100 μM, right).

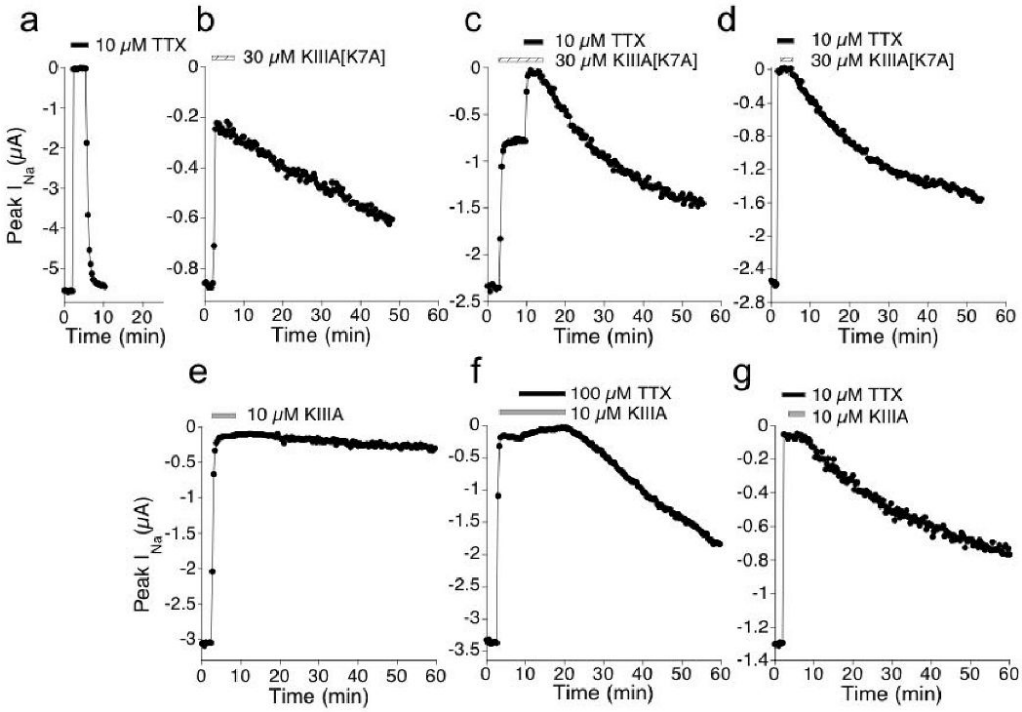

Figure 2.

TTX blocks residual I_{Na} that persists in saturating concentrations of KIIIA[K7A] or KIIIA and accelerates the rate of peptide-washout. Example plots of peak I_{Na} recorded from oocytes during exposure to: TTX (**a**); KIIIA[K7A] (**b**); KIIIA[K7A] followed by KIIIA[K7A]+TTX (**c**); TTX followed by TTX+KIIIA[K7A] (**d**); KIIIA (**e**); KIIIA followed by KIIIA+TTX (**f**); and TTX followed by TTX+KIIIA (**g**). Different oocyte was used in each of panels **b** to **g**, where previous exposure to 10 μM TTX obliterated I_{Na} (not shown, but as in **a**). Presence of 10 or 100 μM TTX is indicated by black bar, 30 μM KIIIA[K7A] by hatched bar, and 10 μM KIIIA by gray bar. In all cases, except **e**, recovery of I_{Na} during toxin-washout could be fit by a single exponential time course (k_{off} values are listed in Table 1). Test pulses were applied at 20 s intervals (see Methods).

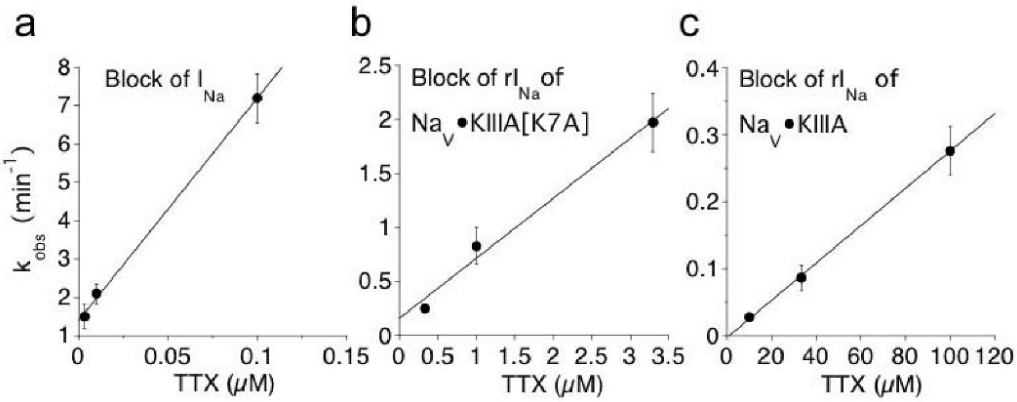

Figure 3.

Rate of TTX-block of control I_{Na} (**a**), residual I_{Na} in 30 μM KIIIA[K7A] (**b**), and in 10 μM KIIIA(**c**) differ radically from each other (note different time scales). Time course of block of rI_{Na} by various [TTX], each fit to a single exponential (not illustrated), provided the observed rate constants (k_{obs}). Plots show k_{obs} for different [TTX]. Relative timing of the exposure to toxin was essentially as in Fig. 2a for Na_V, Fig. 2c for Na_V•KIIIA[K7A], and Fig. 2f for Na_V•KIIIA. Linear regression slope, providing apparent k_{on}, was 58 ± 5.3 $\mu M^{-1}min^{-1}$ (**a**), 0.56 ± 0.08 $\mu M^{-1}min^{-1}$ (**b**), and 0.003 ± 0.0004 $\mu M^{-1}min^{-1}$ (**c**).

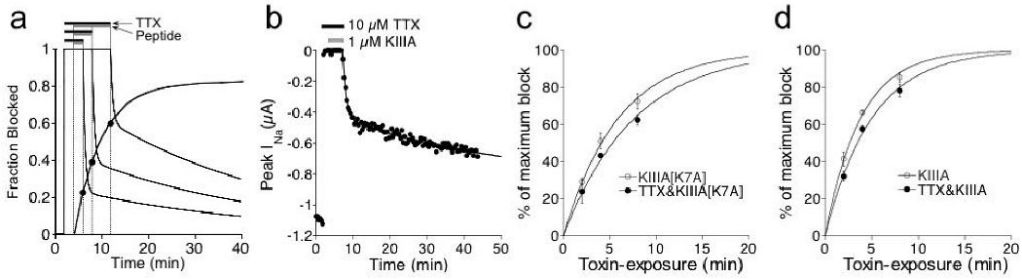

Figure 4.

Apparent on-rate of peptide binding in the presence of TTX was only slightly slower than the rate of block by peptide in the absence of TTX. Level of peptide bound to $Na_V1.2$ in the face of 10 μM TTX was determined by the amount of persistent-block following washout of both toxins. (**a**) Protocol used to determine level of persistent-block by peptide (i.e., formation of Na_V•TTX•peptide). Results from series of three hypothetical experiments are superimposed: oocyte was exposed to TTX for 2 min. followed by exposure to TTX + peptide for 2, 4, or 8 min before washing out both toxins (black bars represent presence of TTX, and gray bars, TTX + peptide). In each case, the washout curve was fit to a double exponential, of which the span and k_{off} of the faster and slower components represent the recovery from block of Na_V•TTX and Na_V•TTX•peptide, respectively. The closed circles represent the span of the slower component and correspond to the closed circles in **c** and **d**. (**b**) Representative results showing peak I_{Na} during exposure to, and following washout of, TTX and KIIIA (black and gray bars, respectively). (**c, d**) Time course for the formation of Na_V • TTX•peptide (closed circles), estimated by the persistent-block produced by 1 μM peptide as described in **a** for different durations of simultaneous-exposure to TTX+peptide (cf., closed circles in **a**), compared with the formation of Na_V • peptide (open circles) simply measured by block produced by 1 μM peptide alone. Data were fit to single exponential curves (solid lines). k_{obs} for formation of Na_V • KIIIA[K7A] and Na_V • TTX • KIIIA[K7A] was 0.17 ± 0.006 and 0.13 ± 0.006 min^{-1}, respectively (**c**). k_{obs} for formation of Na_V • KIIIA and Na_V •TTX • KIIIA was 0.27 ± 0.01 and 0.20 ± 0.008 min^{-1}, respectively (**d**).

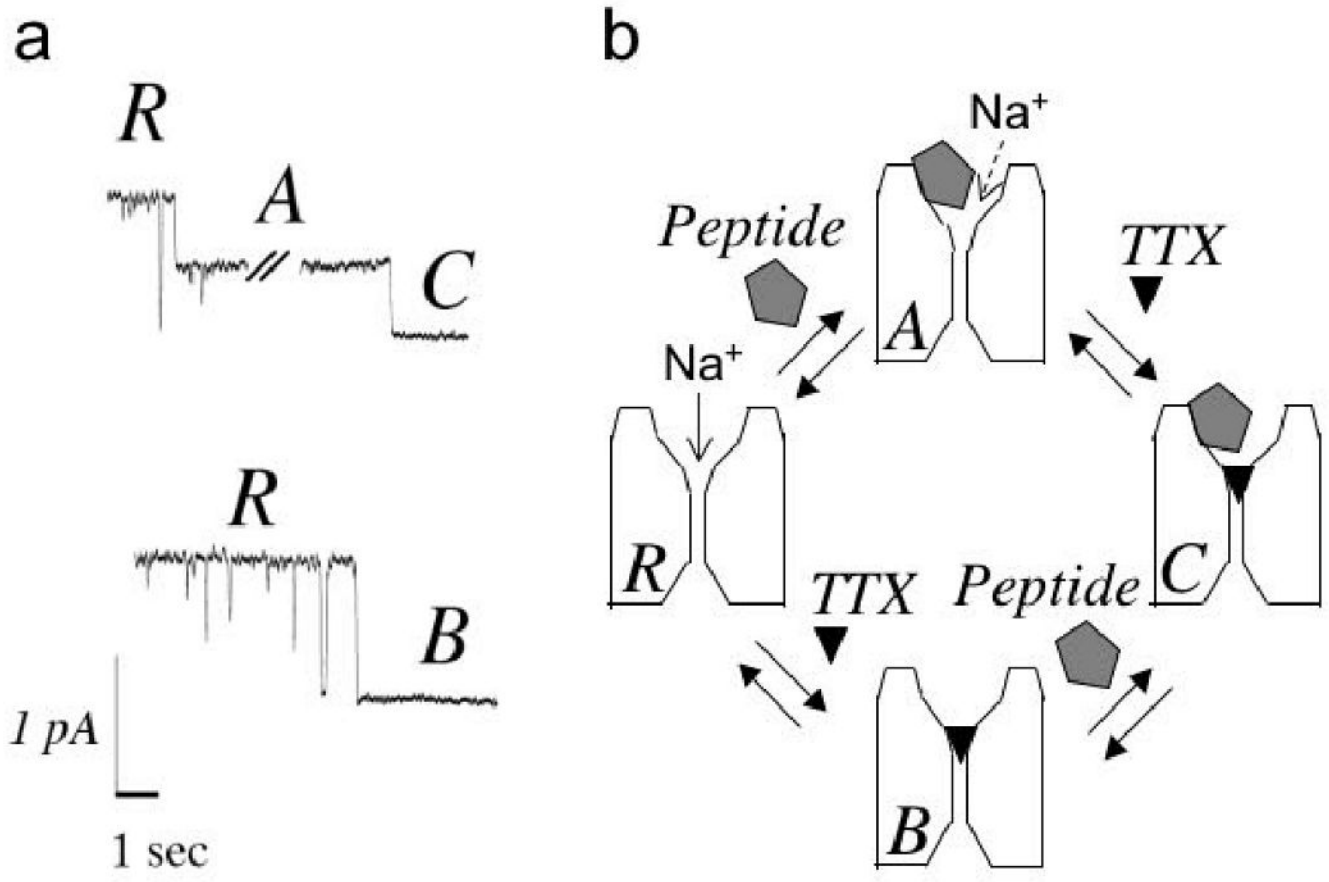

Figure 5.

Single-channel records (**a**) and proposed reaction scheme (**b**). The conductance states "*R*", "*A*", "*B*", and "*C*" in (**a**) correspond to the 4 configurations in (**b**). All putative transitions except "*B*" to "*C*" are illustrated in (**a**); the "*B*" to "*C*" transition would not result in a change in the current level due to complete block by TTX. (**a**) Recordings from a single rat brain sodium channel incorporated into a planar bilayer membrane were obtained as described in Methods. Upper trace: Begins in the "*R*" level (open level, unblocked) in the presence of KIIIA [K7A] (2 μM), and then steps to the partially blocked level "*A*" indicating binding of the peptide. After KIIIA[K7A] binding, TTX concentration was increased to 10 μM, and ~1 minute later, a transition was seen to a fully blocked level "*C*", which we interpret as the bi-liganded state (Na_V•TTX•KIIIA[K7A]). Lower trace, channel block in the presence of TTX (50 nM), without peptide, clearly defines the unblocked open level and fully blocked/closed level "*B*", which shows the same conductance as the bi-liganded state "*C*" shown in the upper trace. (**b**) Reaction scheme consistent with both single-channel and macroscopic results. "*R*" represents ligand-free (fully functional) channel; "*A*", peptide-blocked channel (where residual I_{Na} is indicated by dashed arrow); "*B*", TTX-blocked channel; and "*C*", the ternary (bi-liganded Na_V) complex.

Table 1

Kinetic[a] and equilibrium constants of μ-conotoxins, TTX and toxin-combinations on $Na_V1.2$

Peptide or complex[b]	IC_{50} (nM)	k_{on} ($\mu M^{-1}\cdot min^{-1}$)	k_{off} (min^{-1})	K_d (nM)
KIIIA	N.D.[c]	0.3±0.03	0.0016±0.0016[d]	5.3±5
KIIIA[K7A]	N.D.[c]	0.13±0.006	0.015±0.005	115±38
TTX	12.6 (11.7-13.6)	58±5.3	2.2±0.3	37.9±6
Na_V•KIIIA•TTX			0.017±0.002	
Na_V•TTX•KIIIA			0.02±0.005	
Na_V•KIIIA[K7A]•TTX			0.024±0.004	
Na_V•TTX•KIIIA[K7A]			0.025±0.003	

[a] Kinetic data were obtained as described in Methods, unless otherwise indicated.

[b] The order of the components in a complex indicates the order in which the components were added: for Na_V•KIIIA•TTX, the channel was exposed to KIIIA first, then to a mixture of KIIIA and TTX (see Fig. 2f); for Na_V•TTX•KIIIA, the order was reversed (see Fig. 2g) (the k_{off}'s were the same within experimental error, suggesting the same ternary complex formed)—likewise for Na_V•KIIIA[K7A]•TTX (see Fig. 2c) and Na_V•TTX•KIIIA [K7A] (see Fig. 2d).

[c] When [peptide] near the expected IC_{50} was tested, the reaction was too slow to reach steady-state within the time-frame of the experiment.

[d] Estimated from level of recovery after 20 min and assuming exponential time course. Values in parentheses are 95% confidence interval, and ± value indicates S.D. ($n \geq 3$). k_{on} of KIIIA is as previously reported[11], all other constants were determined in experiments of the present report.

Table 2

Comparison of block of wild-type $Na_V1.2$ *versus* $Na_V1.2$[F385C] by TTX and KIIIA

Ligand	Variable	WT $Na_V1.2$	$Na_V1.2$[F385C]
TTX	**IC_{50}** (μM)	0.013 (0.012-14)[a]	39 (34-44)[c]
KIIIA	**k_{on}** ($\mu M^{-1} \cdot min^{-1}$)	0.3±0.03[a]	0.5±0.06
KIIIA	**k_{off}** (min^{-1})	0.0016±0.0016[a]	0.0047±0.0016[d]
KIIIA	**K_d** (nM)	5±5[a]	9±3
KIIIA	**rI_{Na}** (% of control)	5±3[b]	10±2

[a] From Table 1.

[b] From Fig. 1.

[c] IC_{50} was determined using [TTX] up to 100 μM (at which 72 ± 3% block was observed) and fitting data to the Langmuir isotherm (see Fig. 1 legend) assuming 100% block at saturating [TTX].

[d] Estimated from level of recovery after 20 min and assuming exponential time course. Values in parentheses are 95% confidence interval, and ± value indicates S.D. ($n \geq 3$).